Eur. Phys. J. C 44, 219–226 (2005)
Digital Object Identifier (DOI) 10.1140/epjc/s2005-02366-x

THE EUROPEAN PHYSICAL JOURNAL C

Application of the two-scale model to the HERMES data on nuclear attenuation

N. Akopov[a], L. Grigoryan[⋆], Z. Akopov

Yerevan Physics Institute, Br. Alikhanian 2, 375036 Yerevan, Armenia

Received: 10 February 2005 / Revised version: 7 July 2005 /
Published online: 13 September 2005 –

Abstract. The two-scale model and its improved version were used to perform a fit to the HERMES data for the ν (the virtual photon energy) and z (the fraction of ν carried by hadron) dependences of the nuclear multiplicity ratios for π^+ and π^- mesons electro-produced on two nuclear targets (^{14}N and ^{84}Kr). The quantitative criterion χ^2 was used for the first time to analyze the results of the model fit to the nuclear multiplicity ratios data. The two-parameter's fit gave satisfactory agreement with the HERMES data. Best values of the parameters were then used to calculate the ν and z dependences of the nuclear attenuation for π^0, K^+, K^-, and $\bar{p}$ produced on the ^{84}Kr target, and also make predictions for ν, z, and the Q^2 (the photon virtuality) dependences of the nuclear attenuation data for those identified hadrons and nuclei that will be published by HERMES.

1 Introduction

Studies of hadron production in deep inelastic semi-inclusive lepton–nucleus scattering (SIDIS) offer a possibility to investigate the quark (string, color dipole) propagation in dense nuclear matter and the space-time evolution of the hadronization process. It is well known from QCD that confinement forbids the existence of an isolated color charge (quark, antiquark, etc.). Consequently, it is clear that after the deep inelastic scattering (DIS) of a lepton on the intra-nuclear nucleon, a complicated colorless pre-hadronic system arises. Its propagation in the nuclear environment involves processes like multiple interactions with the surrounding medium and induced gluon radiation. If the final hadron is formed inside the nucleus, it can interact via the relevant hadronic cross section, causing further reduction of the hadron yield [1]. QCD at present cannot describe the process of quark hadronization because of the major role of "soft" interactions. Therefore, the understanding of quark hadronization is of basic importance for the development of QCD. for this purpose we investigate the nuclear attenuation (NA), which is the ratio of the differential multiplicity on a nucleus (A) to that on deuterium (D).

The experimentally measured observable is

$$R_M^h(\nu,z,Q^2)=\frac{\left(\frac{N^h(\nu,z,Q^2)}{N^e(\nu,Q^2)}\right)_A}{\left(\frac{N^h(\nu,z,Q^2)}{N^e(\nu,Q^2)}\right)_{\rm D}},$$

with $N^h(\nu,z,Q^2)$ being the number of semi-inclusive hadrons in a given (ν,z,Q^2) bin, and $N^e(\nu,Q^2)$ being the number of inclusive DIS positrons in the same (ν,Q^2) bin. The experimental data used are one dimensional, which assumes that integration is done over all other kinematic variables.

Presently, there are numerous phenomenological models on the market for the investigation of the NA [2–14]. The two-scale model (TSM) [4] and its improved version (ITSM) is used in this work to perform a fit to the HERMES NA data [15,16]. For a fit procedure we use the high-statistics and therefore a more precise part of the data sample, which includes data for the ν and z dependences of NA for π^+ and π^- mesons on two nuclear targets (^{14}N and ^{84}Kr). The ν and z dependences of NA for π^0, K^+, K^-, and antiproton, produced on the ^{84}Kr target, are described with best values of the parameters obtained from the above-mentioned fit. Then, the set of parameters is used also for the prediction of the ν, z, and Q^2 dependences of NA for the data from those targets that will be published soon by HERMES [17]. The remainder of this paper is organized as follows. In Sect. 2 we briefly recall the TSM. In Sect. 3 we discuss the possibility of the inclusion of the Q^2 dependence in the TSM. In Sect. 4 we describe the scheme we used to improve the TSM, substituting the step-by-step increase of the string–nucleon cross section by a smooth raising function. In Sect. 5 we present the results of the model fit to the HERMES data. Our conclusions are given in Sect. 6.

[a] e-mail: akopoff@mail.desy.de

[⋆] Supported by DESY, Deutsches Elektronen-Synchrotron.

2 The two-scale model

The TSM is a string model which was proposed by EMC [4] and used for the description of their experimental data. The basic formula is

$$R_A = 2\pi \int_0^\infty b\mathrm{d}b \int_{-\infty}^\infty \mathrm{d}x\rho(b,x) \times \left[1 - \int_x^\infty \mathrm{d}x'\sigma^{\mathrm{str}}(\Delta x)\rho(b,x')\right]^{A-1}, \quad (1)$$

where b is the impact parameter, x the longitudinal coordinate of the DIS point, $\rho(b,x)$ the nuclear density function, x' the longitudinal coordinate of the string–nucleon interaction point, $\sigma^{\mathrm{str}}(\Delta x)$ the string–nucleon cross section on a distance $\Delta x = x' - x$ from the DIS point, and A the atomic mass number.

The string models are based on the idea that after DIS the knocked-out (anti)quark does not leave the nucleon remnant, and forms a string (color dipole) with the (anti)quark on the fast and the nucleon remnant on the slow end, while the color string itself consists of gluons. Its longitudinal size must be larger than the transverse size, but cannot be essentially larger than the hadronic size because of confinement. The string can then break down into two strings according to the following scenarios. First, when the quark–antiquark pair from the color field of the string is produced; and second, when the color interaction between the string and the nucleon (lying on its trajectory) has occurred (see for instance [3]). In the "history" of the string there are two time scales which are of interest to us. These are the time scales connected with the production of the first constituent (anti)quark of the final hadron and the interaction of two constituents for the first time. As it has been mentioned above, the model contains two scales (see Fig. 1): τ_{c} (l_{c}) the constituent formation time (length)[1]; and τ_h (l_h) the yo-yo formation time (length). The yo-yo formation means that a colorless system with valence content and quantum numbers of the final hadron is formed, but without its "sea" partons.

In the two-dimensional string models which satisfy the following conditions:
(1) quark–antiquark pairs arising from the vacuum do not have energy;
(2) energy loss of the leading quark on unit length (string tension) is constant (a widely known example is the Lund model), there is a simple connection between τ_h and τ_{c}:

$$\tau_h - \tau_{\mathrm{c}} = z\nu/\kappa\,, \quad (2)$$

where $z = E_h/\nu$, E_h, and ν are the energies of the final hadron and the virtual photon respectively, and κ is the string tension (string constant). Further we will use two different expressions for τ_{c}. The first expression for τ_{c} is obtained for hadrons containing a leading quark [18]:

$$\tau_{\mathrm{c}} = (1-z)\nu/\kappa\,. \quad (3)$$

[1] In relativistic units ($\hbar = c = 1$, where $\hbar = h/2\pi$ is the reduced Planck constant and c the speed of light) $\tau_i = l_i, i = \mathrm{c}, h$ because partons and hadrons move with near-light speeds.

The color string fully spends its energy on a distance of $L = \nu/\kappa$ beginning from the DIS point (see Fig. 1). The last hadron produced from the string is $h = H_1$, which contains a leading quark and carries an energy E_h. At distance L, the energy of the leading quark becomes equal to zero and the whole energy of the hadron is concentrated in another constituent. This constituent collects its energy from the string and will have energy E_h on a distance L only if it was produced on a distance $E_h/\kappa = z\nu/\kappa$ from L. This is reflected in (3). It is important to note that the hadron produced on the fast end of string is not always necessarily the fastest hadron.

The second expression for the average value of τ_{c} used in this paper was obtained in [5, 19] in the framework of the standard Lund model [20]:

$$\tau_{\mathrm{c}} = \int_0^\infty l\mathrm{d}lD_{\mathrm{c}}(L,z,l) \Big/ \int_0^\infty \mathrm{d}lD_{\mathrm{c}}(L,z,l)\,, \quad (4)$$

where $D_{\mathrm{c}}(L,z,l)$ is the distribution of the constituent formation length l of hadrons carrying momentum z. This distribution is

$$D_{\mathrm{c}}(L,z,l) = L(1+C)\frac{l^C}{(l+zL)^{C+1}} \times \left(\delta(l-L+zL) + \frac{1+C}{l+zL}\right)\theta(l)\theta(L-zL-l)\,, \quad (5)$$

where $L = \nu/\kappa$, and $C = 0.3$ is the parameter which controls the steepness of the standard Lund fragmentation function. The path traveled by the string between the DIS and interaction points is $\Delta x = x' - x$. The string–nucleon cross section is

$$\sigma^{\mathrm{str}}(\Delta x) = \theta(\tau_{\mathrm{c}} - \Delta x)\sigma_q + \theta(\tau_h - \Delta x)\theta(\Delta x - \tau_{\mathrm{c}})\sigma_s$$

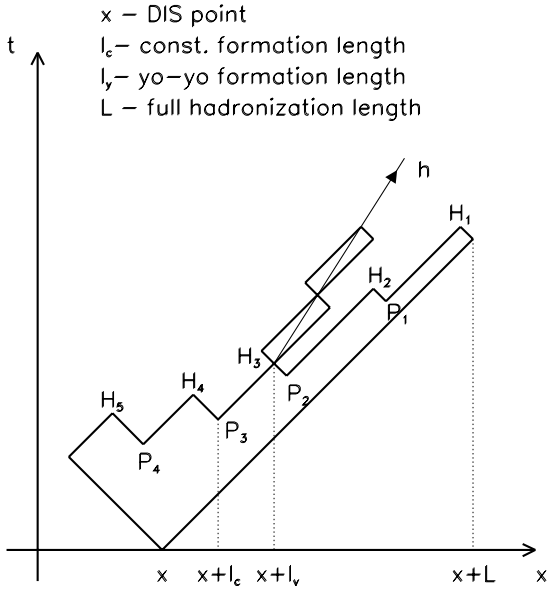

Fig. 1. Space-time structure of hadronization in the string model. The two constituents of the hadron are produced at different points. The constituents of the hadron h are created at the points P_2 and P_3. They meet at H_3 to form the hadron

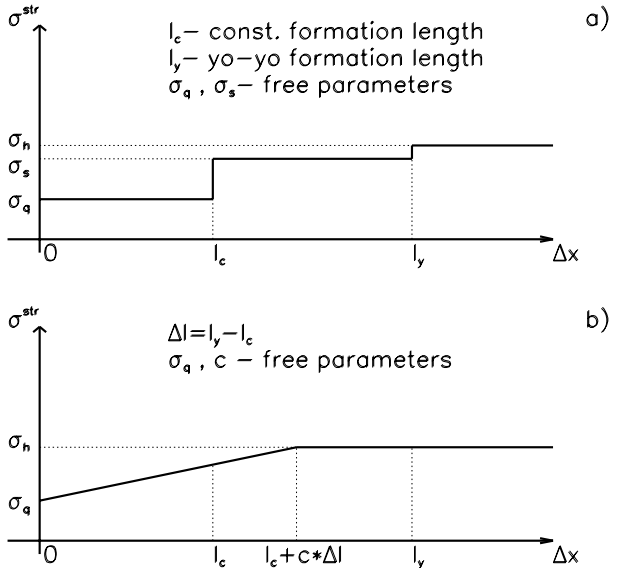

Fig. 2. a The behavior of the string–nucleon cross section as a function of the distance in the TSM. **b** The same as in **a** for ITSM taking into account a more realistic smoothly increasing string–nucleon cross section

$$+\theta(\Delta x - \tau_h)\sigma_h \,, \tag{6}$$

where σ_q, σ_s, and σ_h are the cross sections for the interaction with the nucleon of the initial string, the open string (which means the string containing the first constituent (anti)quark of the final hadron on its slow end) and the final hadron respectively (see Fig. 2a).

It is worthy to add that (1) is written for the case where the nuclear properties of deuterium are neglected. In our calculations we also take into account absorption in deuterium, and use the ratio $R_M^h = R_A/R_{\rm D}$ with R_A as defined in (1).

3 Inclusion of the Q^2 dependence in TSM

In the following discussion two quantities will be used for the virtuality of the string: Q^2 (precise value) for consideration of the Q^2 dependence, and $\hat{Q}^2$ (average value) for consideration of the ν and z dependences. The TSM was introduced in [4] for the description of the ν and z dependences of NA and does not contain a direct Q^2 dependence, while it deals with cross sections measured at average values of Q^2:

$$\sigma_q = \sigma_q(\hat{Q}^2); \qquad \sigma_s = \sigma_s(\hat{Q}^2_{\tau_{\rm c}}) \,, \tag{7}$$

where $\hat{Q}^2$ is average value of Q^2 in the moment of DIS. $\hat{Q}^2_{\tau_{\rm c}} = \hat{Q}^2(\tau_{\rm c})$ is the value of $\hat{Q}^2$ for the open string, or in the time interval $\tau_{\rm c}$ after DIS. $\hat{Q}^2_{\tau_{\rm c}}$ must be smaller than $\hat{Q}^2$, because the string radiates gluons and diminishes its virtuality. QCD predicts the Q^2 dependence of the string–nucleon cross section in the form [21, 22]

$$\sigma_q(Q^2) \sim 1/Q^2; \qquad \sigma_s(Q^2_{\tau_{\rm c}}) \sim 1/Q^2_{\tau_{\rm c}} \,. \tag{8}$$

Using this prediction we can express the cross section for the initial string as follows:

$$\sigma_q(Q^2) = (\hat{Q}^2/Q^2)\sigma_q(\hat{Q}^2) \,. \tag{9}$$

In the same way the expression for the open string cross section can be written as

$$\sigma_s(Q^2_{\tau_{\rm c}}) = (\hat{Q}^2_{\tau_{\rm c}}/Q^2_{\tau_{\rm c}})\sigma_s(\hat{Q}^2_{\tau_{\rm c}}) \,, \tag{10}$$

where $Q^2_{\tau_{\rm c}} = Q^2(\tau_{\rm c})$ is the virtuality of the string in the time interval $\tau_{\rm c}$ after DIS. In order to estimate the ratio of $\hat{Q}^2_{\tau_{\rm c}}/Q^2_{\tau_{\rm c}}$ we adopt the scheme given in [23, 24]. In accordance with this scheme, during time t the quark decreases its virtuality from the initial Q^2 to the value $Q^2(t)$ as follows:

$$Q^2(t) = \nu(t)\frac{Q^2}{\nu(t) + tQ^2} \,, \tag{11}$$

where $\nu(t) = \nu - \kappa t$. The calculations show that for the HERMES kinematics ($1.2 < Q^2 < 9.5\,{\rm GeV}^2$ and $\hat{Q}^2 = 2.5\,{\rm GeV}^2$), the values for the ratio $\hat{Q}^2_{\tau_{\rm c}}/Q^2_{\tau_{\rm c}}$ are close to 1 (for $\tau_{\rm c}$ in the form of (3), it changes in the region 0.97–1.04, and in the form of (4) in the region 0.92–1.12). This ratio is not dependent on ν, while it depends on z and Q^2, and only at z larger than 0.7 for $\tau_{\rm c}$ in the form of (4), it deviates from 1 by more than 10%.

However, in the case of a Q^2 dependence, just the average value of z in a given Q^2 bin should be taken into account. Since the multiplicity as a function of z diminishes at large z values, the average value of z cannot be greater than 0.5 depending on the kinematics of the experiment. Calculations show that the inclusion of a factor $\hat{Q}^2_{\tau_{\rm c}}/Q^2_{\tau_{\rm c}}$ instead of unity leads to a maximal deviation in the R_M^h value for the lowest and highest Q^2, which in the case of HERMES kinematics corresponds to 2% at $Q^2 = 1\,{\rm GeV}^2$ and 2.5% at $Q^2 = 10\,{\rm GeV}^2$. Taking into account the above-mentioned arguments we can conclude that the constant approximation for σ_s is quite reasonable in the HERMES kinematics.

4 Improved version of the two-scale model

In the TSM the string–nucleon cross section is a function which jumps in the points $\Delta x = \tau_{\rm c}$ and τ_h. In reality the cross section increases smoothly until it reaches the size of the hadronic cross section, hence it makes direct sense to improve the model in order to reflect this (see Fig. 2).

We introduce the parameter c ($0 < c < 1$) in order to take into account the well-known fact that the string starts to interact with the hadronic cross section soon after the creation of the first constituent quark of the final hadron and before the creation of a second constituent. The string–nucleon cross section starts to increase from the DIS point, and reaches the value of the hadron–nucleon cross section at $\Delta x = \tau$. However, in that case one cannot extract the exact form of $\sigma^{\rm str}$ from perturbative QCD, at least in the region of $\Delta x \sim \tau$. This means that some model for the shrinkage–expansion mechanism has to be introduced. We

use four versions for the definition of $\sigma^{\rm str}$. Two of them were taken from [25].

Let us briefly discuss the physical reason behind the linear or quadratic dependence of the cross section on $\Delta x/\tau$, which will be presented below [26]. The QCD lattice calculations show that the confinement radius is much smaller than the mean hadronic radii. Consequently the color field in the hadrons is located in tubes with a transverse size much smaller than the longitudinal one. The valence quarks and diquarks are placed at the end-points of these tubes. In case of inelastic scattering, the interacting hadron-tubes intersect in the impact-parameter plane. The probability of the crossing of the tubes is proportional to their length. This means that $\sigma^{\rm str}$ increases proportional to $\Delta x/\tau$. In the naive parton model, the inelastic cross section of a hadron with a nucleon is proportional to the transverse area which is filled in by its partons, i.e. $\sigma^{\rm str}$ increases proportionally to $(\Delta x/\tau)^2$.

The first version of the definition of $\sigma^{\rm str}$ is based on quantum diffusion:

$$\sigma^{\rm str}(\Delta x) = \theta(\tau-\Delta x)[\sigma_q + (\sigma_h-\sigma_q)\Delta x/\tau] + \theta(\Delta x-\tau)\sigma_h\,, \quad (12)$$

where $\tau = \tau_{\rm c} + c\Delta\tau$, $\Delta\tau = \tau_h - \tau_{\rm c}$.

The second version follows from the naive parton case:

$$\sigma^{\rm str}(\Delta x) = \theta(\tau-\Delta x)[\sigma_q + (\sigma_h-\sigma_q)(\Delta x/\tau)^2] + \theta(\Delta x-\tau)\sigma_h\,. \quad (13)$$

Two other expressions for $\sigma^{\rm str}$ were also used [2,6]:

$$\sigma^{\rm str}(\Delta x) = \sigma_h - (\sigma_h-\sigma_q)\exp\left(-\frac{\Delta x}{\tau}\right) \quad (14)$$

and

$$\sigma^{\rm str}(\Delta x) = \sigma_h - (\sigma_h-\sigma_q)\exp\left(-\left(\frac{\Delta x}{\tau}\right)^2\right)\,. \quad (15)$$

One can easily note that at $\Delta x/\tau \ll 1$ the expressions (14) and (15) turn into (12) and (13), respectively.

At first glance it may seem that the ITSM, as opposed to the TSM, is actually a one-scale model. But one must note that τ is a function of the two scales $\tau = (1-c)\tau_{\rm c} + c\tau_h$ whereas the parameter c regulates the inclusion of each scale into τ.[2]

5 Results

In this work we have formulated one of possible improvements of the TSM and performed a fit to the HERMES data [15,16] using the TSM and ITSM. Only the NA data for the ν and z dependences for π^+ and π^- mesons on ^{14}N and ^{84}Kr nuclei were used for the actual fit. For each measured bin the values of $\hat{z}$ (averaged over the given ν bin) in the case of the ν dependence, and $\hat{\nu}$ in the case of a z dependence were taken from the experimental data, whereas the use of these values allows one to avoid the problem of additional integration over z and ν in (1). The string tension (string constant) was fixed at a static value determined by the Regge trajectory slope [24,27]

$$\kappa = 1/(2\pi\alpha'_R) = 1\,{\rm GeV/fm}\,. \quad (16)$$

The nuclear density functions (NDF) were used as follows: for deuterium the hard core deuteron wave functions from [32] were used. For ^{4}He and ^{14}N, the shell model [28] is used, according to which four nucleons (two protons and two neutrons) fill the s-shell, and the other $A-4$ nucleons are on the p-shell:

$$\rho(r) = \rho_0\left(\frac{4}{A} + \frac{2}{3}\frac{(A-4)}{A}\frac{r^2}{r_A^2}\right)\exp\left(-\frac{r^2}{r_A^2}\right)\,, \quad (17)$$

where $r_A = 1.31\,{\rm fm}$ for ^{4}He and $r_A = 1.67\,{\rm fm}$ for ^{14}N.

For ^{20}Ne, ^{84}Kr, and ^{131}Xe the Woods–Saxon distribution was used:

$$\rho(r) = \rho_0/(1+\exp((r-r_A)/a))\,. \quad (18)$$

These three sets of NDF's were used for the fitting with the following corresponding parameters: the first set [29], $a = 0.54\,{\rm fm}$,

$$r_A = (0.978 + 0.0206A^{1/3})A^{1/3}\,{\rm fm}\,. \quad (19)$$

The second set [30], $a = 0.54\,{\rm fm}$,

$$r_A = \left(1.19A^{1/3} - \frac{1.61}{A^{1/3}}\right)\,{\rm fm}\,, \quad (20)$$

and the third set [31], $a = 0.545\,{\rm fm}$,

$$r_A = 1.14A^{1/3}\,{\rm fm}\,, \quad (21)$$

where the values of ρ_0 are determined from the normalization condition:

$$\int {\rm d}^3 r\rho(r) = 1\,. \quad (22)$$

The parameter a is practically the same for all three sets; the radius r_A for the third set is larger by approximately 6% than the one for the first and second sets. Two expressions for $\tau_{\rm c}$ were used for the fitting procedure – (3) and (4). For $\sigma^{\rm str}(\Delta x)$ one expression in TSM, (6), and four different expressions in ITSM, (12)–(15), were used. The values of σ_h (hadron–nucleon inelastic cross section) used in the fit were set equal to $\sigma_{\pi^+} = \sigma_{\pi^-} = 20\,{\rm mb}$. Two parameters were determined from the fit. In the case of TSM they are σ_q and σ_s, and σ_q and c in the case of ITSM. The meaning of the parameter c was introduced in Sect. 4.

Afterwards, using the best fit parameters, different predictions were made for the ν, z, and Q^2 dependences for those identified hadrons and nuclei that will be published by HERMES [17].

[2] We encourage the readers to form their own opinion on this definition.

Table 1. The TSM: the best values for the fitted parameters and χ^2/DOF ($N_{\rm exp} = 58$, $N_{\rm par} = 2$)

		$\tau_{\rm c}$ (3)			$\tau_{\rm c}$ (4)	
NDF	σ_q (mb)	σ_s (mb)	χ^2/DOF	σ_q (mb)	σ_s (mb)	χ^2/DOF
(19)	5.3 ± 0.01	17.1 ± 0.08	4.3	4.2 ± 0.01	16.6 ± 0.07	2.3
(20)	5.5 ± 0.01	17.7 ± 0.08	4.5	4.3 ± 0.01	17.3 ± 0.07	2.4
(21)	5.8 ± 0.01	18.3 ± 0.08	4.8	4.4 ± 0.01	18.1 ± 0.07	2.6

Table 2. The ITSM: $\tau_{\rm c}$ (3). The best values for the fitted parameters and χ^2/DOF ($N_{\rm exp} = 58$, $N_{\rm par} = 2$)

		$\sigma^{\rm str}$ (12)			$\sigma^{\rm str}$ (13)	
NDF	σ_q (mb)	c	χ^2/DOF	σ_q (mb)	c	χ^2/DOF
(19)	0.46 ± 0.02	0.32 ± 0.03	1.4	3.5 ± 0.01	0.23 ± 0.002	1.9
(20)	0.62 ± 0.01	0.31 ± 0.01	1.7	3.7 ± 0.01	0.22 ± 0.02	2.1
(21)	0.78 ± 0.02	0.30 ± 0.03	1.8	3.9 ± 0.01	0.21 ± 0.003	2.3
		$\sigma^{\rm str}$ (14)			$\sigma^{\rm str}$ (15)	
NDF	σ_q (mb)	c	χ^2/DOF	σ_q (mb)	c	χ^2/DOF
(19)	1.1 ± 0.01	0.15 ± 0.03	2.1	3.7 ± 0.01	0.15 ± 0.02	2.3
(20)	1.3 ± 0.02	0.15 ± 0.03	2.4	3.9 ± 0.01	0.14 ± 0.02	2.6
(21)	1.5 ± 0.02	0.14 ± 0.03	2.8	4.1 ± 0.01	0.14 ± 0.02	2.9

Table 3. The ITSM: $\tau_{\rm c}$ (4). The best values for the fitted parameters and χ^2/DOF ($N_{\rm exp} = 58$, $N_{\rm par} = 2$)

		$\sigma^{\rm str}$ (12)			$\sigma^{\rm str}$ (13)	
NDF	σ_q (mb)	c	χ^2/DOF	σ_q (mb)	c	χ^2/DOF
(19)	0.0 ± 0.001	0.56 ± 0.02	4.6	0.97 ± 0.01	0.17 ± 0.002	1.6
(20)	0.0 ± 0.002	0.53 ± 0.02	4.3	1.0 ± 0.02	0.17 ± 0.02	1.5
(21)	0.0 ± 0.002	0.49 ± 0.006	4.0	1.1 ± 0.02	0.16 ± 0.02	1.6
		$\sigma^{\rm str}$ (14)			$\sigma^{\rm str}$ (15)	
NDF	σ_q (mb)	c	χ^2/DOF	σ_q (mb)	c	χ^2/DOF
(19)	0.0 ± 0.001	0.24 ± 0.02	3.0	1.5 ± 0.02	0.103 ± 0.02	1.5
(20)	0.0 ± 0.002	0.21 ± 0.02	2.9	1.7 ± 0.02	0.096 ± 0.02	1.6
(21)	0.0 ± 0.002	0.18 ± 0.02	2.8	1.8 ± 0.02	0.089 ± 0.02	1.8

The results of the performed fit are presented in Tables 1, 2, and 3.

Table 1 shows the best values of the fitted parameters, their errors and χ^2/DOF for the TSM. Tables 2 and 3 show these values for the ITSM. The only difference between Tables 2 and 3 is the form of $\tau_{\rm c}$ that was used.

Results for the TSM (Table 1) are qualitatively close to the results of [4]. The values of $\sigma_q \ll \sigma_h$ and σ_s are approximately equal to σ_h, while σ_q obtained in the present analysis is larger than the same in [4], because $\hat{Q}^2$ for the HERMES kinematics is smaller than at the EMC experiment. The lowest (best fit) value of χ^2/DOF = 1.4 was obtained for the ITSM (see Table 2) for NDF by (19), $\sigma^{\rm str}(\Delta x)$ as in (12) and the constituent formation time $\tau_{\rm c}$ in the form of (3). Values close to χ^2/DOF = 1.5, were obtained for the two other versions of the ITSM with the constituent formation time $\tau_{\rm c}$ in the form of (4) (see Table 3) for NDF, (20), $\sigma^{\rm str}$, (13), and NDF, (19), $\sigma^{\rm str}$, (15).

For the TSM (Table 1) the best fit value of χ^2/DOF = 2.3 was obtained for NDF as in (19), and the constituent formation time $\tau_{\rm c}$ in the form of (4). The results for NA, calculated with the best values of the fit parameters from the ITSM and TSM, for the ν and z dependences of the produced charged pions on the ^{14}N and ^{84}Kr targets are presented on Fig. 3. One can see that where precise experimental data are available, it is useful to perform not only a visual comparison of the models to the data but also use the correct quantitative comparison using the χ^2 criterion. Indeed, even though a visual comparison hardly allows one to determine which model better describes the data, the value of χ^2/DOF for the ITSM is substantially smaller. Furthermore, the NA for the hadrons produced on the ^{84}Kr target (but not included in the fit), were calculated. In Fig. 4 one can see the ν and z dependences for these identified hadrons. The values of σ_h that were used are as follows: $\sigma_{\pi^0} = \sigma_{K^-} = 20\,{\rm mb}$, $\sigma_{K^+} = 14\,{\rm mb}$, and

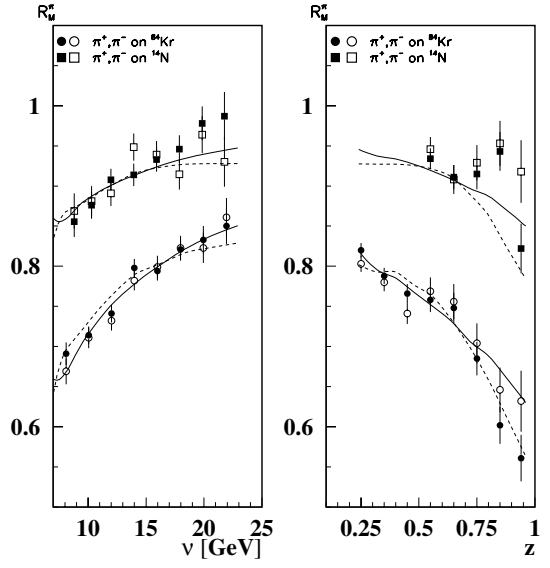

Fig. 3. Hadron multiplicity ratio R of charged pions for the ^{14}N [15] and ^{84}Kr [16] nuclei as a function of ν (left panel) and z (right panel). The solid curves correspond to the ITSM with NDF, (17), for ^{14}N and NDF, (19), for ^{84}Kr and $\sigma^{\rm str}$, (12), with $\tau_{\rm c}$ in the form (3) for the values of the parameters $\sigma_q = 0.46\,{\rm mb}$, $c = 0.32$. The dashed curves correspond to the TSM with the same NDF for nuclei and $\tau_{\rm c}$ in the form (4) for the values of parameters $\sigma_q = 4.2\,{\rm mb}$, $\sigma_s = 16.6\,{\rm mb}$. These data were included in the fit and the curves were obtained as a result of the fit

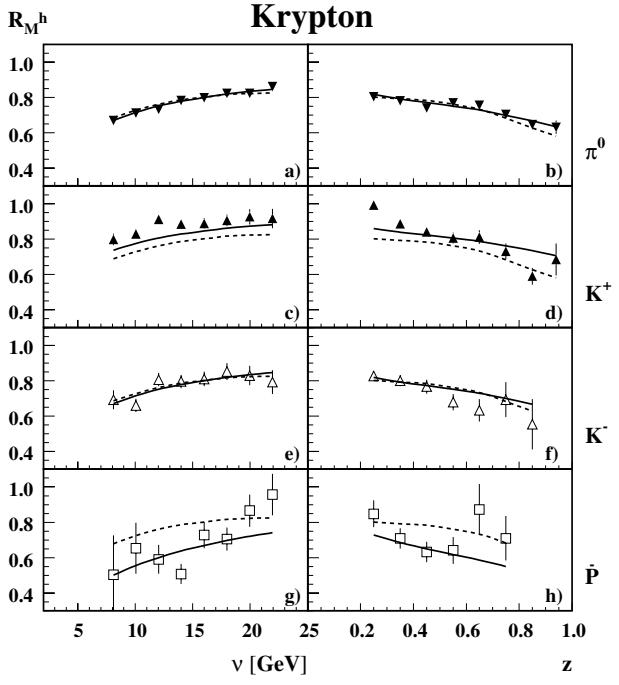

Fig. 4. Hadron multiplicity ratio R of different species of hadrons produced on the ^{84}Kr target [16] as a function of ν (left panel) and z (right panel). These data were not included in the fit. The curves are calculated with the best fit parameters described in the caption of Fig. 3

$\sigma_{\bar{p}} = 42\,{\rm mb}$. The curves correspond to the ITSM and TSM model calculations with the best set of parameters.

Satisfactory agreement is achieved for all of the considered hadrons. The proton was not included in these calculations due to the following reasons. Among others, the proton is quite unique, because it already exists in the nucleus before the DIS act. All other hadrons are mainly produced as a result of fragmentation of the knocked-out quark and only the proton has more complicated production mechanisms: from the remnant of the nucleon on which the DIS takes place, from the fragmentation of the knocked-out quark. Also, another possible scenario could be the color interaction of the other nucleons with the string.

Figure 5 shows the results of the TSM and ITSM in comparison with the experimental data for the NA of charged hadrons on the ^{63}Cu target [4] performed in the region of ν and Q^2 values higher than in the HERMES kinematics. In order to compare with the EMC data we have redefined σ_q to the $\hat{Q}^2_{\rm EMC} \sim 10.6\,{\rm GeV}^2$ according to the expression (9). We would like to discuss Fig. 5 in detail for several reasons. First, the EMC data for the NA are for charged hadrons and it is not quite clear which value should be used for σ_h. We use the same σ_h as for the pions, due to the simple assumption that at higher energies mainly the pions are produced; moreover, it has been checked that the NA weakly depends on σ_h at higher energies. Secondly, we see that the high energy data can be used to distinguish, or choose more precisely, different versions of the models. In particular, the EMC data seem to agree better with

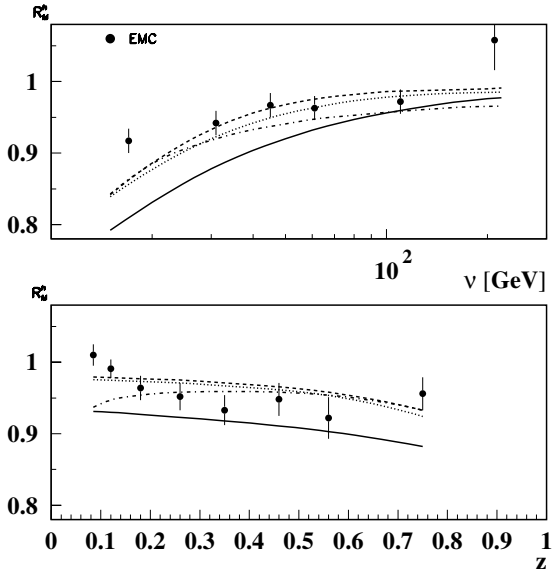

Fig. 5. The ratio R for charged hadrons for ^{63}Cu [4] as a function of ν (upper panel) and z (lower panel). The solid, dashed, and dotted curves correspond to three sets of parameters with the minimal values of χ^2/DOF in case of ITSM (see Tables 2 and 3): solid NDF, (19), $\sigma^{\rm str}$, (12), $\tau_{\rm c}$, (3), $\sigma_q = 0.46\,{\rm mb}$, $c = 0.32$, $\chi^2/{\rm DOF} = 1.4$; dashed NDF, (20), $\sigma^{\rm str}$, (13), $\tau_{\rm c}$, (4), $\sigma_q = 1.0\,{\rm mb}$, $c = 0.17$, $\chi^2/{\rm DOF} = 1.5$; dotted NDF, (19), $\sigma^{\rm str}$, (15), $\tau_{\rm c}$, (4), $\sigma_q = 1.5\,{\rm mb}$, $c = 0.103$, $\chi^2/{\rm DOF} = 1.5$. The dashed-dotted curves correspond to the best set of parameters in case of TSM (see Table 1): NDF, (19), $\tau_{\rm c}$, (4), $\sigma_q = 4.2\,{\rm mb}$, $\sigma_s = 16.6\,{\rm mb}$, $\chi^2/{\rm DOF} = 2.3$

the case where the constituent formation time τ_c is used as in (4).

The investigation of NA is not complete, until one includes also the Q^2 dependence into the consideration. This was already discussed in Sect. 3. On the figures that show the results for the Q^2 dependence it is convenient to represent the NA ratio versus the inverse of Q^2, because of the connection of this dependence with higher twist effects. Indeed, from (9), (6), (12)–(15), and (1) we can conclude that in first approximation the expansion over the degrees of $1/Q^2$ for the NA ratio can be represented in the form $R_A = a + b/Q^2$, where b is negative. One has to note that for the calculation of the Q^2 dependence, $\sigma_q(Q^2)$ was used instead of σ_q, whereas the corresponding expression is given by (9). Using the best set of parameters obtained by performing a fit to the published HERMES data [15, 16] for TSM and ITSM, we present the predictions for the new set of the HERMES data [17] for ^{4}He (Fig. 6), ^{20}Ne (Fig. 7), ^{84}Kr (Fig. 8), and ^{131}Xe (Fig. 9). Let us finally briefly discuss the nuclear matter distribution functions. For medium and heavy nuclei the preferable NDF is the Woods–Saxon distribution. However, there is some freedom in the choice of the parameters themselves, therefore we have included three sets of parameters, (19)–(21), in order to study the uncertainty of the fitting procedure related to the NDFs.

6 Conclusions

(1) The HERMES data for the ν and z dependences of NA of the π^+ and π^- mesons on two nuclear targets (^{14}N and ^{84}Kr) were used to perform the fit of the TSM and ITSM.
(2) The χ^2 criterion was used for the first time for such a kind of analysis, to perform a comparison with the NA data.
(3) A two-parameter fit demonstrates satisfactory agreement with the HERMES data. A minimum χ^2 (best fit) was obtained for the ITSM, including the expression (12) for $\sigma^{\rm str}$ and (3) for τ_c. The published HERMES data do not give the possibility to make a choice between the expressions (12)–(15) for the $\sigma^{\rm str}$, as well as to make a distinct preference of the definitions (3) or (4) for τ_c, because they give close values of χ^2.

Preferable NDF's are the sets (19) and (20) as described in Sect. 5, because with these NDF's, the lowest values of χ^2 were obtained for both TSM and ITSM. Moreover, considering ten versions of different forms for τ_c and $\sigma^{\rm str}$ in TSM and ITSM, only two of them with the relative minimal χ^2 values correspond to NDF (21) (see Tables 1, 2, and 3).
(4) More precise data that are expected from HERMES [17] will provide essentially better conditions for the choice of preferable version of the model in terms of the different expressions for $\sigma^{\rm str}$ and τ_c.
(5) In all versions we have obtained that $\sigma_q \ll \sigma_h$. This indicates that at an early stage of the hadronization process color transparency takes place.
(6) We do not include in the consideration the NA of protons, because in this case additional mechanisms connected

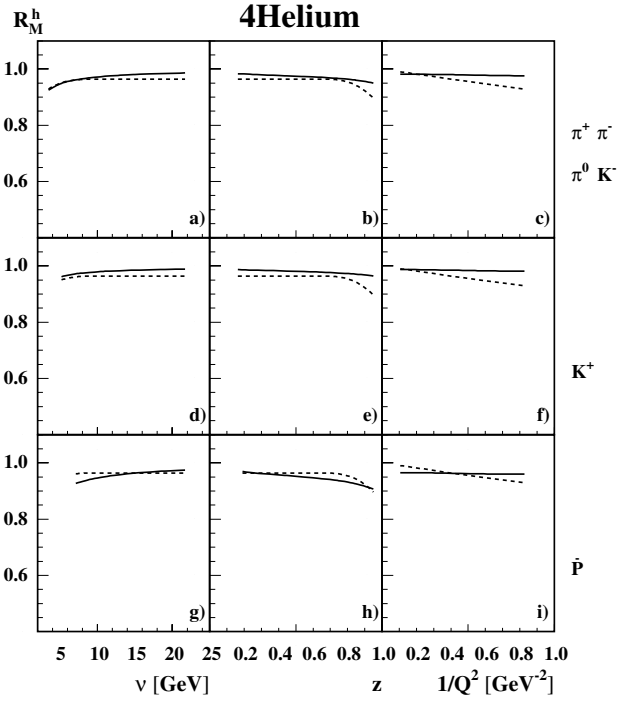

Fig. 6. The ratio R for different species of hadrons for the ^{4}He target as a function of ν (left), z (central), and Q^2 (right panel). NDF has been taken in the form (17). The solid and dashed curves calculated with best fit parameters for ITSM and TSM, respectively (see the caption of Fig. 3). Calculations performed for extended kinematics of HERMES [17]: for mesons $\nu > 2\,\mathrm{GeV}$, $z > 0.1$, $Q^2 > 1\,\mathrm{GeV}^2$; for antiprotons $\nu > 4\,\mathrm{GeV}$, $z > 0.1$, $Q^2 > 1\,\mathrm{GeV}^2$

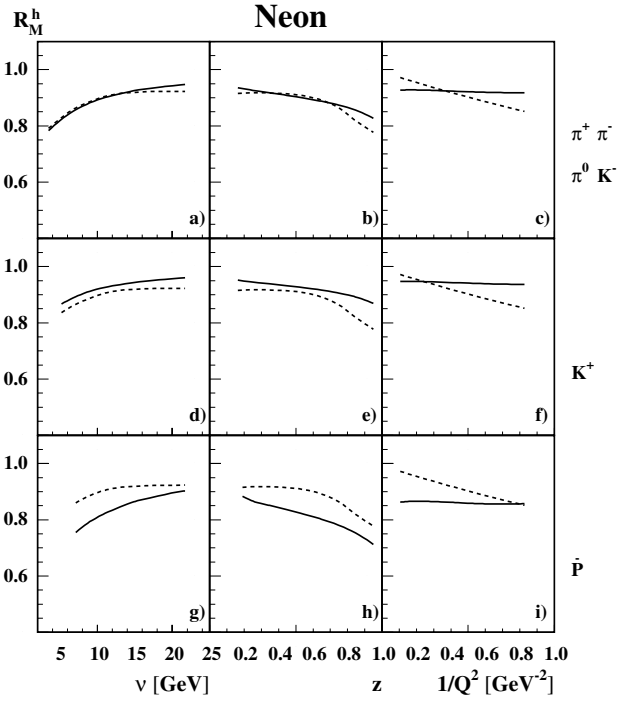

Fig. 7. The same as described in the caption of Fig. 6 for the ^{20}Ne target

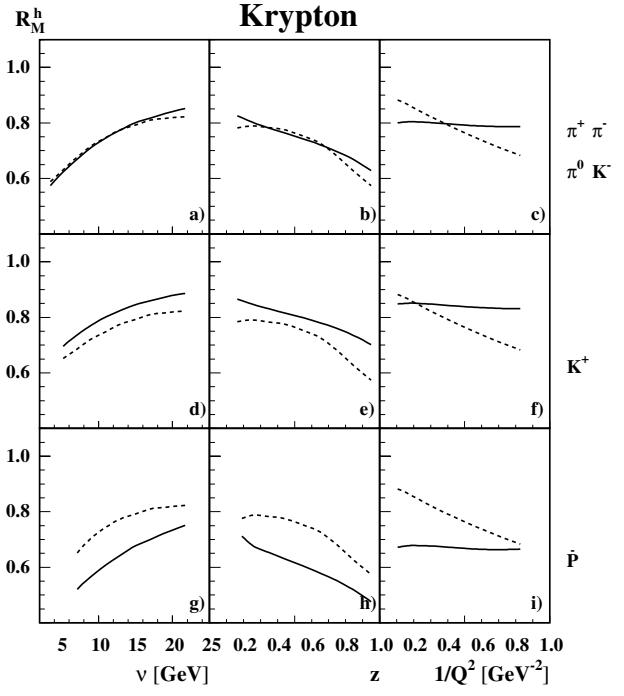

Fig. 8. The same as described in the caption of Fig. 6 for the ^{84}Kr target. The NDF are taken in the form (19)

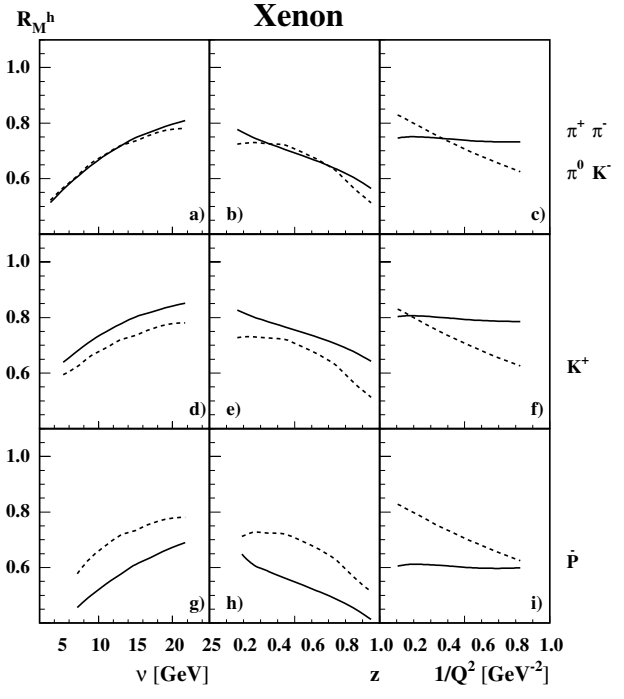

Fig. 9. The same as described in the caption of Fig. 6 for the ^{131}Xe target. The NDF are taken in the form (19)

with the color interaction (string-flip) and final hadron rescattering become essential (see for instance [3, 5]).

Acknowledgements. We would like to acknowledge P. Di Nezza and E. Aschenauer for helpful discussions and suggestions. We also thank G. Elbakian as well as many other colleagues from the HERMES Collaboration for fruitful discussions.

References

1. N. Nikolaev, Z. Phys. C **5**, 291 (1980); V. Anisovich et al., Nucl. Phys. B **133**, 477 (1978); G. Davidenko, N. Nikolaev, Nucl. Phys. B **135**, 333 (1978)
2. A. Bialas, Acta Phys. Pol. B **11**, 475 (1980)
3. M. Gyulassy, M. Plumer, Nucl. Phys. B **346**, 1 (1990)
4. J. Ashman et al., Z. Phys. C **52**, 1 (1991)
5. J. Czyzewski, P. Sawicki, Z. Phys. C **56**, 493 (1992)
6. R. Badalyan, Z. Phys. C **55**, 647 (1992)
7. N. Akopov, G. Elbakian, L. Grigoryan, hep-ph/0205123
8. T. Falter, W. Cassing, K. Gallmeister, U. Mosel, Phys. Lett. B **594**, 61 (2004); Phys. Rev. C (in press), nucl-th/0406023
9. J. Dias De Deus, Phys. Lett. B **166**, 98 (1986)
10. A. Accardi, V. Muccifora, H.J. Pirner, Nucl. Phys. A **720**, 131 (2003)
11. F. Arleo, JHEP **11**, 44 (2002); Eur. Phys. J. C **30**, 213 (2003)
12. X.-N. Wang, X. Guo, Nucl. Phys. A **696**, 788 (2001); E. Wang, X.-N. Wang, Phys. Rev. Lett. **89**, 162301 (2002)
13. B. Kopeliovich, J. Nemchik, E. Predazzi, Proceedings of the workshop on Future Physics at HERA, edited by G. Ingelman, A. De Roeck, R. Klanner, DESY, 1995/1996, vol. 2, p. 1038 (nucl-th/9607036); B. Kopeliovich et al., hep-ph/0311220
14. D.J. Dean et al., Phys. Rev. C **46**, 2066 (1992)
15. A. Airapetian et al., Eur. Phys. J. C **20**, 479 (2001)
16. A. Airapetian et al., Phys. Lett. B **577**, 37 (2003)
17. G. Elbakyan [HERMES Collaboration], in: Proceedings of the DIS 2003, St. Petersburg, 2003, edited by V.T. Kim, L.N. Lipatov, p. 597
18. B. Kopeliovich, Phys. Lett. B **243**, 141 (1990)
19. A. Bialas, M. Gyulassy, Nucl. Phys. B **291**, 793 (1987); T. Chmaj, Acta Phys. Pol. B **18**, 1131 (1987)
20. B. Andersson et al., Phys. Rep. **97**, 31 (1983)
21. B. Kopeliovich, B. Povh, Proceedings of the workshop on Future Physics at HERA, edited by G. Ingelman, A. De Roeck, R. Klanner, DESY, 1995/1996, vol. 2, p. 959
22. K.Golec-Biernat et al., Phys. Rev. D **59**, 014017 (1998)
23. B. Kopeliovich et al., Hadron Structure '92 Proceedings Stara Lesna, Czecho-Slovakia, September 6–11, 1992, p. 164
24. B. Kopeliovich, J. Nemchik, preprint JINR E2-91-150 (1991); preprint of INFN-ISS 91/3(1991) Roma
25. G. Farrar et al., Phys. Rev. Lett. **61**, 686 (1988)
26. B. Kopeliovich, J. Nemchik, L. Litov, Int. J. Mod. Phys. E **2**, 767 (1993)
27. T. Sjostrand, L. Lonnblad, S. Mrenna, hep-ph/0108264; LU TP 01-21
28. L. Elton, Nuclear sizes (Oxford University Press, 1961), p. 34
29. A. Bialas et al., Phys. Lett. B **133**, 241 (1983)
30. A. Bialas et al., Nucl. Phys. B **291**, 793 (1987)
31. A. Capella et al., Phys. Rev. D **18**, 3357 (1977)
32. R.V. Reid, Ann. Phys. (New York) **50**, 411 (1968)